Predictor Antennas in Action

Joachim Björsell, Mikael Sternad
Signals and Systems, Uppsala University
PO Box 534, SE-751 21 Uppsala, Sweden
Email: {joachim.bjorsell,mikael.sternad}@angstrom.uu.se

Michael Grieger
AIRRAYS - Wireless Solutions Dresden, Germany
Email: michael.grieger@airrays.com

***Abstract*—Connected vehicles in large numbers will be expensive in terms of power and bandwidth unless advanced transmit schemes are employed. These would rely on channel state information at transmitter (CSIT), which rapidly becomes outdated for fading vehicular channels. We here evaluate the predictor antenna concept, that solves this problem by using antennas on the outside of vehicles, with one extra antenna in front of the others. Its estimated channel is a scaled prediction for the channels encountered by rearward antennas when they reach that position.**

We evaluate this concept on a large set of channel sounding measurements from an urban environment. Recent investigations of the correlations of these measurements indicate that the average normalized mean squared errors (NMSEs) of the complex valued channel predictions should be around -10 dB for prediction horizons in space of up to 3 wavelengths. This represents an extension of the attainable prediction horizon by an order of magnitude, as compared to Kalman or Wiener extrapolation of past channel measurements. It represents an accuracy that would enable e.g. accurate massive multiple input multiple output (MIMO) downlink beamforming to vehicles.

We here perform predictions on a subset of the measurements with good channel-to-estimation error power ratio (SNR). The approximate true channels are here available and we evaluate the performance on a validation data set. The results confirm that the distribution of the NMSE, over all investigated propagation environments, is close to that obtained by correlation-based models and outperforms the use of outdated channel measurements.

I. INTRODUCTION

Vehicular users and Intelligent Transport Systems are important drivers for the development of 5G wireless access [1], [2]. Future wireless networks will need to support a large number of connected vehicles. This could become very costly in terms of transmission resources due to the required coverage and the rapid channel variation caused by short-term fading: Power, bandwidth and antenna resources are required to combat the effects of fading by adequate power margins and diversity.

More power- and spectrally efficient transmission requires channel state information at transmitter (CSIT). This would, for example, enable the use of fast link adaptation, fine-grained channel-aware scheduling, adaptive transmit beamforming, and Coordinated Multipoint (CoMP) transmission. In particular, downlink multiple input multiple output (MIMO) transmission that uses large numbers of antenna elements (Massive MIMO and coherent joint processing CoMP) would increase the spectral efficiency, the power efficiency, the area coverage/transmit range as well as the link stability [3], [4]. However, channel measurements would become outdated for vehicular users due to the rapid channel variations and the latencies involved in transmission control (obtaining, distributing and using channel measurements). CSIT that captures the short-term fading is not used efficiently today for vehicular users.

978-1-5386-3531-5/17/$31.00

Could channel prediction provide reliable CSIT for vehicular users? That depends on the carrier frequency, the prediction horizon and the velocity. The short-term fading of radio channels can to some extent be predicted, based on past measurements of the channel [5]–[7]. A required prediction horizon of L seconds (due to the transmission control latency) is equivalent to a prediction over space expressed in terms of carrier wavelengths:

$$Lf_d = \frac{Lv}{\lambda} = \frac{Lvf_c}{c} \quad \text{[wavelengths]} \,, \tag{1}$$

where f_d is the maximal Doppler frequency in Hz, v is the vehicle velocity in m/s, λ is the carrier wavelength in m, c is the speed of light and f_c is the carrier frequency. The relation is illustrated by Fig. 1 for $L = 5$ ms (left) and $L = 1$ ms (right).

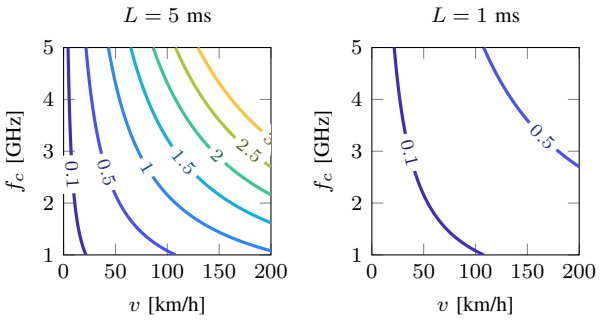

Fig. 1. Required prediction range in carrier wavelengths corresponding to a prediction horizon of 5 ms (left) and 1 ms (right), as a function of the vehicle velocity and the carrier frequency.

The transmission control delay that determines L is at least 5 ms in 4G LTE systems today. It could be reduced towards 1 ms in latency-optimized 5G new radio

standards but will likely be higher if multi-site cooperative transmission is utilized. Transmission to vehicles that is not designed specifically for short distances is likely to mainly use frequencies above 1 GHz and below 6 GHz, with new spectral bands around 3.5 GHz being of interest for 5G. A channel predictor for vehicular users in evolved 4G and 5G systems would therefore need to handle prediction horizons in space of $0.5\,\lambda - 3\,\lambda$.

Even the best available schemes for channel prediction that are based on past measurements, namely Kalman and Wiener prediction, do not provide adequate accuracy for $Lf_d > 0.2\,\lambda - 0.3\,\lambda$ for non-line-of-sight channels [6], [8], [9]. Methods for longer prediction horizons have been suggested, but they fail to work when evaluated on channel measurements.[1]

We here focus on improving the predictability of the vehicular channel by proposing a modified antenna system at the vehicle. We have called this framework the *predictor antenna concept*:

- First, we assume that external antennas are placed on the outside of the vehicle, in this case on the roof. This will in itself improve the channel by avoiding the outdoor-to-indoor propagation loss. In-vehicle users can then be served by local (vehicular) relay nodes [10], or by WLAN.
- Second, we propose to place one extra antenna at sufficient distance $\Delta d \geq L_{\max} v_{\max}$ ahead in the direction of movement relative to the nearest antenna behind it, where $L_{\max}$ is the longest required prediction horizon and $v_{\max}$ is the maximal vehicle velocity, see Fig. 2. This antenna is called the predictor antenna.

The electromagnetic field forms a standing wave pattern, and the vehicle moves through this pattern. Reference signal-based filter estimates or smoothing estimates of the channel to the predictor antenna can be used to estimate this pattern. By sampling the wavefield in advance, the estimated channel can then be used to predict the channels to be encountered by the rearward antennas when they reach that position. The prediction accuracy is with this scheme no longer limited by the channel correlation properties in time as measured at one single antenna. It will instead depend on the correlation between the channel at the predictor antenna and the channel encountered later by a rearward antenna, when it has reached that position. Thereby, CSIT can be obtained for e.g. all antennas of a linear array that are placed behind the predictor antenna.[2]

[1]One such class of methods is based on the extrapolation of a sparse set of channel impulse response components that are assumed to vary as sinusoids. Unfortunately, the resulting algorithms tend to perform somewhat worse than Kalman predictors that are based on estimated autoregressive models, when applied to measured data. One such comparison can be found in [4].

[2]The predictor antenna itself can be utilised for uplink and downlink communication, but its channel state will be less well predicted than that of other antennas located behind it.

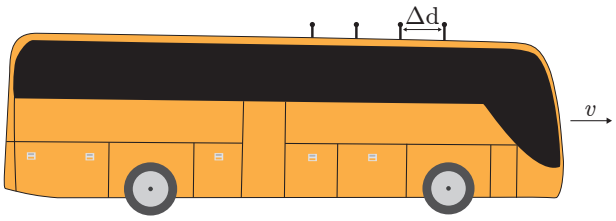

Fig. 2. Multiple antennas on the vehicle roof, where the one in front may act as a predictor antenna.

The predictor antenna concept was proposed in [8], and preliminary experimental correlations were reported therein for two measurement locations, using two dipole antennas on the roof of a vehicle. A similar scheme for time division duplex (TDD) systems was proposed in [11]. Much higher correlations, but still only from two measurement locations, were obtained in [12] for two monopole antennas placed on a flat metal sheet on a vehicle roof.

In [13], the correlation statistics was assessed for a very large set of measurements at vehicular velocities at 2.53 GHz, obtained in a multitude of urban fading environments in downtown Dresden, Germany. These measurements are described in Section IV-A below.

A large part of the measurements contain a significant amount of noise, for which the true, noise-free, channels are unavailable. Therefore, we in [13] assessed the performance indirectly, via a correlation-based statistical model that is outlined in Section II below. The measured correlations indicate that on average over all measurement locations, a normalized mean squared error (NMSE) of -11 dB can be obtained for prediction horizons of $0.25\,\lambda$ and -8.5 dB for horizons of $3\,\lambda$. This represents an order-of-magnitude increase of the attainable prediction horizon as compared to the extrapolation of time-series.

In the present paper, we focus on a subset of our measurements that have good channel-to-estimation error power ratio (SNR). The estimated channels for the rearward antennas can here approximately be regarded as the true channels, which can be compared to the predictions. We perform and evaluate predictor-antenna based channel prediction, using an algorithm outlined in Section III. The predictor is adjusted based on data from an *estimation interval* and predictions are then performed in a later *prediction interval*. Results are presented in Section IV and are compared to the estimates from the statistical performance model of [13].

II. PERFORMANCE MODEL

A. Predictor Design and NMSE Performance

The complex scalar channel h_m for the main antenna, at L seconds into the future, is predicted by multiplying the already estimated, and appropriately delayed, channel

h_p at the predictor antenna by a complex-valued coefficient a_h according to

$$\hat{h}_m(t+L) = a_h \hat{h}_p(t+L-\Delta t|t) \ . \tag{2}$$

Here, t is the current time, $\hat{h}_p(t+L-\Delta t|t)$ is a smoothing estimate of h_p based on noisy measurements up to t and Δt is the time difference between the predictor antenna and main antenna passing through the same position in space. Prediction horizons $L \leq \Delta t$ can be accommodated without extrapolating $\hat{h}_p$.

Noisy estimates of the main antenna channel and of the predictor antenna channel are assumed unbiased and are here described by the following simplified model

$$\hat{h}_p(t|t-L+\Delta t) \triangleq y_p(t) = h_p(t) + e_p(t), \tag{3}$$

$$y_m(t) = h_m(t) + e_m(t), \tag{4}$$

where the channels, $h_p(t)$ and $h_m(t)$, and the estimation errors, $e_p(t)$ and $e_m(t)$, are assumed zero mean. Then, the mean squared error (MSE)-optimal predictor gain a_h in (2) can be derived assuming that the estimation errors are uncorrelated with the channels and are mutually uncorrelated, $\mathrm{E}[e_m(t)e_p^*(t-\tau)]=0$.

The MSE-optimal predictor gain is then given by

$$a_h = \frac{c}{\sigma_{y_p}^2}, \tag{5}$$

where

$$\begin{aligned} c &= \mathrm{E}[h_m(t)h_p^*(t-\Delta t)] = \mathrm{E}[h_m(t)y_p^*(t-\Delta t)] \\ &= \mathrm{E}[y_m(t)y_p^*(t-\Delta t)] \end{aligned} \tag{6}$$

is the maximal correlation between the two channels and $\sigma_{y_p}^2 = \mathrm{E}[y_p(t)y_p^*(t)]$ is the average power of the predictor antenna channel estimates.

The theoretical NMSE $\mathrm{E}\,|\hat{h}_m(t)-h_m(t)|^2 / \mathrm{E}\,|h_m(t)|^2$, given the prediction coefficient in (5), is

$$\mathrm{NMSE} = 1 - |b|^2 \frac{\gamma_p}{(1+\gamma_p)} \ . \tag{7}$$

where $\gamma_p = \sigma_p^2/\sigma_{e_p}^2$ is the channel-to-estimation error power ratio (here denoted SNR) of the predictor antenna channel and $\sigma_{e_p}^2$ is the power of the estimation error $e_p(t)$ in (3). The normalized physical correlation b between the predictor antenna and the main antenna is defined by

$$b = \frac{c}{\sigma_m \sigma_p}, \tag{8}$$

where σ_m and σ_p are the standard deviations of $h_m(t)$ and $h_p(t)$. This normalized correlation lies in the interval $b \in [-1,1]$. Ideally, $b=1$, but the correlation will be lower in practice. The decorrelation could be caused by the movement of the vehicle itself which affects the wavefield, reflections from moving nearby vehicles, and also lateral and curved motion of the vehicle which affect the antenna paths, so that they do not coincide.

The theoretical NMSE (7) is derived in [13] and is visualized in Fig. 3.

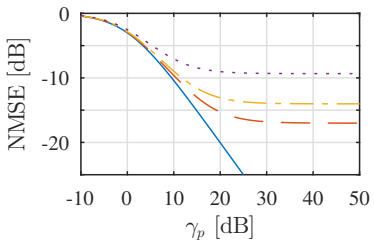

Fig. 3. The theoretical NMSE as a function of the channel-to-estimation error power ratio (SNR) of the predictor channel measurements, γ_p, by (7). The different lines show the relation for the physical correlations, $b=1$, solid line (——), $b=0.99$, dashed line (– –), $b=0.98$, dashed-dotted line (–·–·–) and $b=0.94$, dotted line (·····). Note the saturation of the NMSE at high γ_p when $b<1$.

B. Practical Issues

To obtain a prediction (2) according to the theory above, reference-signal based estimates of the predictor antenna channel can be used. These can be filtered or smoothed to reduce the estimation error in (3). Estimates of a_h according to (5) and of Δt in (2) are also required.

We assume that the radio environment around one position in space is stationary during short intervals. From this assumption, which will be investigated and validated in Section IV, it follows that the correlation c between antennas by (6) should be fairly constant during the same interval. This would allow the predictor antenna concept to be practically implemented by estimating the prediction gain a_h (5) from measurements in the first part of the interval, the estimation interval. The predictor can then be applied according to (2) during a following prediction interval.

The delay Δt in (2) is directly related to the movement of the vehicle. For a constant velocity v, $\Delta t = \Delta d/v$ where Δd is the antennas distance, which is assumed known. The velocity of the vehicle and Δt can therefore be estimated from the correlations peak of $\mathrm{E}[y_m(t)y_p^*(t-\tau)]$, which should occur at $\tau = \Delta t = \Delta d/v$.

III. PREDICTOR ALGORITHM

Based on the discussion in Subsection II-B, we here outline an algorithm of low computational complexity. It consists of a slow scale part and a fast scale part. An overview is shown in Fig. 4.

The slow scale part estimates the prediction coefficient a_h (5) and the velocity v from buffered channel measurements from the predictor antenna and the other antennas. The prediction coefficient is estimated from the maximum antenna correlation and the velocity from the time offset between the antennas at which the correlation is maximized [13]. The slow scale part also selects coefficients of a lowpass finite impulse response (FIR) filter which is applied at the fast time scale to suppress high-frequency estimation errors in $y_p(t)$ and $y_m(t)$ above an estimated Doppler spectral bandwidth, see the discussion below. The parameters a_h, v and

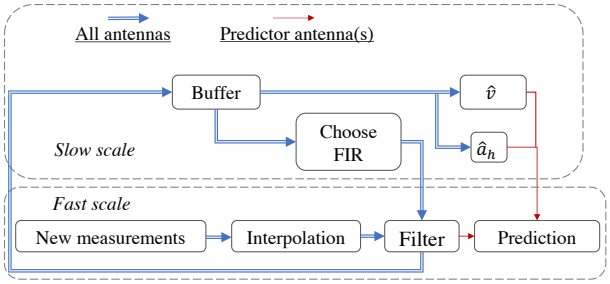

Fig. 4. Flow chart of the main components of the proposed channel prediction algorithm.

filter coefficients are utilized by the fast scale processing during the subsequent prediction interval after which new parameters are estimated by the slow scale part.

The fast scale part interpolates and filters the channels from all antennas and then predicts the channels of the main antennas. Channel interpolation is optionally performed e.g. with spline interpolation to provide a dense and evenly sampled sequence on which the latest adjusted FIR filter can be applied. Filtered predictor antenna channel estimates are used to predict all the main channels L seconds later, by (2). The filtered measurements for all relevant antennas are also copied to the buffer to be used at the next iteration of the slow scale part.

We suggest the use of a lowpass FIR filter of order M with linear phase and unit gain in its passband. In [13], the adjustment of the passband to a measured Doppler spectrum is discussed. Such a filter introduces a delay of $M/2$ samples so it represents a smoother: It has to be applied to measurements $M/2$ samples in advance of the time position of the output. (With a filter with unit passband gain and no net phase shift, the models (3), (4) will then be reasonable for the smoothed estimates.) According to (2), the smoothing lag of $M/2$ samples should not exceed a time interval $\Delta t - L$ when filtering the predictor antenna signal, so the order M of the filter for $h_p(t)$ should be adjusted to the required prediction horizon L.

The combined length of the estimation interval and the following prediction interval should not extend beyond the duration for which the radio environment is stationary as this would reduce the antenna correlation.

The proposed algorithm also requires an initiation process (not shown in Fig. 4). During start-up, one slow scale iteration is required to generate the first slow-scale estimates based on buffered unfiltered measurements.

IV. RESULTS

A. Channel Measurements

The measurements were obtained by driving in downtown Dresden, Germany, with velocities between 0 km/h to 50 km/h. The physical layer parameters that were used are in close compliance with the 3GPP/LTE standard. Since the focus of the current paper is on channel estimation and prediction, only the demodulation reference symbols are evaluated. The channel was measured in the uplink direction using demodulation reference symbols transmitted every 0.5 ms by roof-mounted antennas on the vehicle.

The orthogonal frequency division multiplexing (OFDM) signals, transmitted at 2.53 GHz with 5.4 MHz bandwidth and 15 kHz subcarrier spacing, were simultaneously received and recorded at up to 16 base stations (BSs) located on five sites with up to six-fold sectorization, located 100 m - 1000 m from the vehicle. Each BS was equipped with a two element, cross-polarized KATHREIN 80010541 antenna which has 58° horizontal and 6.1° vertical half power beam width. Time and frequency synchronization of the BSs was done through GPS fed reference normals.

A linear array of four monopole antennas was positioned on the roof of a Volkswagen T4 van in a straight line in the forward-backward direction as shown in Fig. 5. Different antenna distances $\Delta d = \{0.25, 0.5, 1, 2, 3\}\,\lambda$ were used during different measurement campaigns. A metal sheet was used below the antennas in order to have an idealized local surrounding that was independent of the particular type of vehicle.

At the BSs, snapshots of 640 ms duration of the digital received base band signal were stored after down-conversion, analogue-digital conversion, sample rate conversion, and filtering. One snapshot was captured about every minute. All other receiver algorithms such as synchronization, carrier frequency offset compensation, OFDM demodulation and channel estimation were applied offline.

The reference signals from the four antennas of the vehicle used separate regularly spaced sets of 15 kHz subcarriers, with reference signals from each antenna placed on every 4:th subcarrier.[3] With a channel estimation period of 0.5 ms, this resulted in 1280 channel estimates over time on each of 90 subcarriers, each separated by 60 kHz, per snapshot and antenna.

The measurements were affected by hardware impairments such as gain imbalances on different transmit/receiver paths and phase noise. Thus, a compound channel including hardware effects, antenna effects, and the wireless channel was measured.

The channel measurements were obtained in a wide variety of propagation environments, including narrow and wide roads with traffic, intersections, dense urban environments and residential areas.

[3]That different antennas use reference signals at different subcarriers will cause a decorrelation between the predictor antenna channel and the measured channels at the rearward antennas. This decorrelation is small between adjacent antennas, much smaller than the decorrelation by other causes. The effect on the results below is a small increase of the attained NMSE.

Fig. 5. The Volkswagen T4 van on the left hand side and zoomed into the antenna array on the roof on the right hand side.

B. Channel Measurement Selection

Four subsets of the measurements were removed in the study performed here.

- Some measurements were affected by distortions of unknown cause, that generate periodical spikes in the Doppler spectra.
- Second, measurements at vehicle velocity $v = 0$ were not used.
- Third, only measurements sets where at least 350 time samples are sampled after the main antenna has reached the initial position of the predictor antenna were used.
- Finally, the performance evaluation is based on the approximation $h_m(t) = y_m(t)$. Therefore only measurements with SNR ≥ 10 dB (before filtering) for all antennas were used.

The resulting numbers of available, relevant and utilized measurements (measurement location-base station pairs) are shown in Table I. The evaluation in [13] was performed for a larger set, denoted "Long" in Table I, where only the first three subsets were removed.

TABLE I
NUMBER OF MEASUREMENTS FOR DIFFERENT ANTENNA DISTANCES Δd

Campaign	Available	Relevant†	Long*	SNR ≥ 10 dB
$\Delta d = 0.25\,\lambda$	459	115	115	77
$\Delta d = 0.5\,\lambda$	490	305	305	207
$\Delta d = 1\,\lambda$	519	355	355	220
$\Delta d = 2\,\lambda$	577	358	348	265
$\Delta d = 3\,\lambda$	543	346	322	221

† Measurements for vehicle velocities $v > 0$ and with the variance of the high-frequency tails of the Doppler spectra less the 0.5 dB.
* Measurements that fulfil † and with velocities so that at least 350 time samples are sampled after the main antenna has reached the initial position of the predictor antenna.

C. Algorithm Performance

The algorithm described in Section III was applied to the measurement set described in Subsection IV-A. No interpolation was applied to the measurements, as the channel sampling (0.5 ms) is already regular and dense.

Half of the available measurements, 0.32 s, are used as the estimation interval and the other half as the prediction interval.

All pairs of adjacent vehicle antennas were used as predictor antenna - main (rearward) antenna pairs. The errors in our predictions are measured as the differences between the predictions and the FIR smoothed channel measurements of the rearward antenna at the corresponding position. FIR smoothers of order 20 were applied to both the predictor antenna and the main antenna channel estimates. The FIR smoothing improved the SNR of the channel by approximately 9 dB in general for our measurements, so the SNR $\gamma_m = \sigma_m^2/\sigma_{e_m}^2 \geq 19$ dB for most utilized measurements. Prediction NMSE estimates above -16 dB were therefore only little perturbed by remaining estimation errors for the rear antenna.

Fig. 6 shows the NMSE distribution when the prediction antenna is applied on the 220 measurements selected in Subsection IV-B for antenna distance $\Delta d = 1\,\lambda$. The channels at all subcarriers are predicted individually. The NMSE performance is evaluated by four different methods:

1) Optimal: A statistical method based on the optimal predictor coefficient. Using the theory in [13], we calculate correlation-based estimates of the NMSE that should be attained when using an optimal data-based prediction coefficient.[4] We will refer to this case as the optimal case.

2) Theory: A statistical method that includes the effects of nonstationarity between the estimation interval (the first half of the measurement set) and the prediction interval (the second half). The optimal prediction coefficient estimated within the prediction interval differs from the prediction coefficient that can be estimated in the estimation interval. This corresponds to a reduction of prediction performance. We refer to this case as the theoretical case.

The nominal prediction horizon for the optimal and theory case is $1\,\lambda$. (As no actual predictions are produced by these methods, we do not have any defined prediction horizon in time.) The antenna distance $1\,\lambda$ allows for predictions of up to λ/v s in time.

3) Simulation: The performance of the algorithm in Section III using prediction horizons of 8 ms and 24 ms. We will refer to this case as the simulation case.

4) Outdated: Uses the latest channel measurement from the main antenna as prediction, $\hat{h}_m(t+L) = y_m(t)$.

Fig. 6 shows that there are only small difference between the theory case and the simulation. Both performing slightly worse than the optimal case. These results shows that the predictor antenna concept is practically implementable as estimating the prediction coefficient in advance (Theory and Simulation) does not in general reduce the prediction accuracy significantly, as compared to using the optimal one (Optimal).

[4]While the corresponding results in [13] were based on the entire length of 0.64 s of the available measurement sets, the present ones are based on statistics from the second half only.

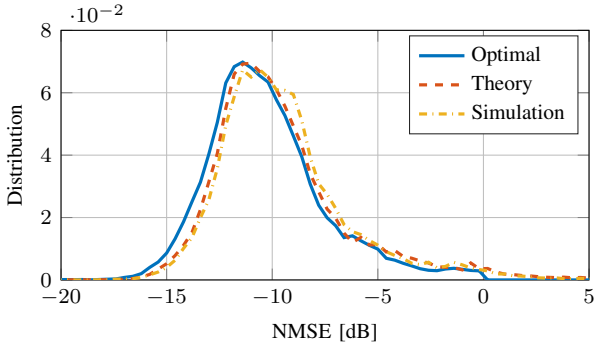

Fig. 6. NMSE distribution for measurement sets with antenna distance $\Delta d = 1\,\lambda$ and prediction horizon $L = 8$ ms for the theoretically optimal predictor coefficient (——), theoretically pre-estimated predictor coefficient (- - -) and simulated predictions (-·-·-).

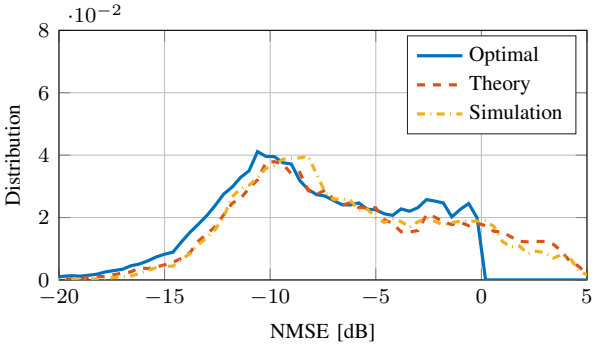

Fig. 8. NMSE distribution for measurement sets with antenna distance $\Delta d = 3\,\lambda$ and prediction horizon $L = 24$ ms for the theoretically optimal predictor coefficient (——), theoretically pre-estimated predictor coefficient (- - -), simulated predictions (-·-·-).

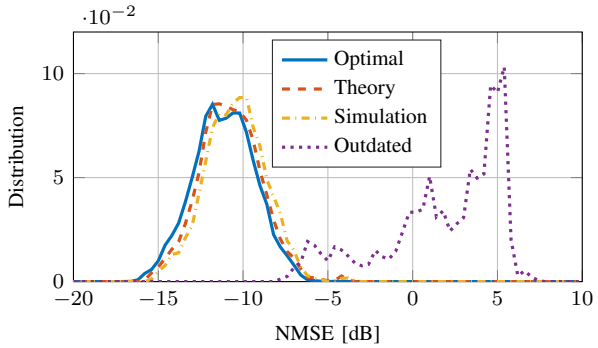

Fig. 7. NMSE distribution for measurement sets with antenna distance $\Delta d = 1\ \lambda$, prediction horizon $L = 8$ ms and $v > 25$ km/h for the theoretically optimal predictor coefficient (——), theoretically pre-estimated predictor coefficient (- - -), simulated predictions (-·-·-) and outdated channel measurements (·····).

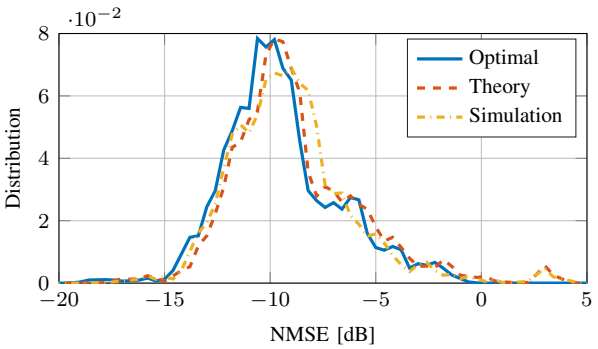

Fig. 9. NMSE distribution for measurement sets with antenna distance $\Delta d = 3\,\lambda$, prediction horizon $L = 24$ ms and $v > 25$ km/h for the theoretically optimal predictor coefficient (——), theoretically pre-estimated predictor coefficient (- - -), simulated predictions (-·-·-).

In [13] it was found that the right-hand tails of the NMSE distribution were almost eliminated when looking at measurements at which the velocity was 25 km/h or higher. In Fig. 7, we see the same NMSE distribution as in Fig. 6 but only for the measurements at which the velocity is 25 km/h or higher. Almost all of the predictions with an NMSE above -7 dB have here disappeared.[5] The figure also shows the uselessly bad NMSE obtained when the outdated channel measurements are used as 8 ms predictions.

The results in Fig. 6 and Fig. 7 are based on measurement with an antenna separation of $\Delta d = 1\,\lambda$ and can provide a prediction horizon in time of at least 8 ms for velocities up to 50 km/h at 2.53 GHz. The corresponding NMSE distributions for the 221 utilized measurements with antenna separation of $\Delta d = 3\,\lambda$ are shown in Fig. 8 and Fig. 9. These measurement provide a prediction horizon of at least 24 ms up to 50 km/h.

[5]The cause of the reduced performance in some of the cases at lower velocities is under current investigation. It should not be a major problem as there are other solutions that work well for low velocities, for example Kalman predictions.

Although the shape of the NMSE distribution is different for the measurements with $\Delta d = 3\,\lambda$ as compared to $\Delta d = 1\,\lambda$, the trends are the same between the methods and also the effect of placing a lower limit on velocities. This also applies to measurements with $\Delta d = \{0.25, 0.5, 2\}\,\lambda$ (not shown here), for which statistics for the optimal case was presented in [13].

V. DISCUSSION AND CONCLUSIONS

We have evaluated the use of predictor antennas directly on a large set of channels that were obtained by channel sounding in different urban propagation environments. We found that the method works well at medium vehicular velocities of 25-50 km/h for OFDM channels at 2.53 GHz in non-line-of-sight as well as line-of-sight environments. The results confirm that the distribution of the NMSE is close to that indicated by the correlation-based model that was introduced in [13].

The obtained prediction accuracy, typically a NMSE of -13 dB to -7 dB, is of a quality that could support many important adaptive transmit methods, but not all schemes that require accurate CSIT. For example, it

would not support single-antenna link adaptation that uses very high order modulation.

Still, the obtained accuracy will support the most important envisioned schemes that promise large gains. In particular, as illustrated in [2], the use of coherent downlink transmission from massive antenna arrays would greatly increase both the power efficiency and the spectral efficiency when serving connected vehicles. It is here of interest that coherent transmit beamforming is quite robust to channel estimation errors, and can utilize imperfect CSIT. The NMSE of a channel formed by maximum ratio transmit beamforming that uses N antennas with equal average channel powers and equal channel estimation error accuracy will be a factor $1/N$ of the individual channel NMSEs [14]. For example, if we predict downlink channels from 64 antenna elements with the here obtained typical average NMSEs of -10 dB, the combined beamformed downlink transmit channel should be known with an NMSE of approximately -28 dB.

The predictor antenna scheme is quite flexible, and can be used in both TDD and frequency division duplex (FDD) systems.

In FDD systems, the downlink channel would be estimated based on downlink reference signals.

For TDD downlinks, the predictor antenna would transmit uplink reference signals and the downlink channels could be obtained at the base station by channel reciprocity. The downlink frames, where no uplink reference signals can be received, should then not be too long. A downlink frame duration corresponding to a movement of more than 0.4 wavelength in space will generate difficulties for the channel interpolation, unless advanced interpolation schemes are used. This is under current investigation.

To summarize, the predictor antenna concept has been found to work well, when using a rather straightforward implementation with low complexity. With such antenna systems, connected vehicles could be served in a spectrally efficient and power efficient way by 5G wireless infrastructure.

ACKNOWLEDGMENTS

We thank the 5G Lab at TU Dresden (Prof. Gerhard Fettweis) for providing the test-bed hardware and software that was used for these measurements. The data analysis was supported by Orange Labs, under contract F03131.

REFERENCES

[1] "5G Automotive vision" A. Kwoczek et. al. 5G Partnership Project White Paper, Oct. 2015. https://5g-ppp.eu/wp-content/uploads/2014/02/5G-PPP-White-Paper-on-Automotive-Vertical-Sectors.pdf

[2] D.-T. Phan-Huy, M. Sternad, T. Svensson, W. Zirwas, B. Villeforceix, F. Karim and S.-E. El-Ayoubi, "5G on board: How many antennas do we need on connected cars?" *IEEE Globecom 2016 Workshop on 5G RAN Design*, Washington DC, Dec. 2016.

[3] F. Rusek, D. Persson, B.K. Lau, E.G. Larsson, T.L. Marzetta, O. Edfors and F. Tufvasson, "Scaling up MIMO: Opportunities and channelges with very large arrays," *IEEE Signal Processing Magazine*, vol. 30, no. 1, Jan. 2013.

[4] V. Jungnickel, K. Manolakis,, W. Zirwas, B. Panzner, V. Braun, M. Lossow, M. Sternad, R. Apelfröjd and T. Svensson, "The role of small cells, coordinated multipoint and massive MIMO in 5G," *IEEE Communications Magazine*, vol. 52, no. 5, pp. 44-51, May 2014.

[5] T. Ekman, A. Ahlén and M. Sternad, "Unbiased power prediction on Rayleigh fading channels," *IEEE Vehicular Technology Conference VTC2002-Fall*, Vancouver, Canada, Sept. 2002.

[6] T. Ekman, *Prediction of Mobile Radio Channels: Modeling and Design.* Ph.D. Thesis, Signals and Systems, Uppsala Univ., 2002. Available: www.signal.uu.se/Publications/pdf/a023.pdf

[7] A. Duel-Hallen, "Fading channel prediction for mobile radio adaptive transmission systems," *Proc. of the IEEE*, vol. 95, no. 12, pp. 2299-2313, Dec. 2007.

[8] M. Sternad, M. Grieger, R. Apelfröjd, T. Svensson, D. Aronsson and A. Belen Martinez, "Using "predictor antennas" for long-range prediction of fast fading moving relays," *IEEE Wireless Communications and Networking Conference (WCNC)*, Paris, April 2012

[9] D. Aronsson, *Channel Estimation and Prediction for MIMO OFDM Systems - Key Design and Performance Aspects of Kalman-based Algorithms.* Ph.D. Thesis, Signals and Systems, Uppsala University, March 2011. www.signal.uu.se/Publications/pdf/a112.pdf

[10] Y. Sui, J. Vihrälä, A. Papadogiannis, M. Sternad, W. Yang and T. Svensson, "Moving cells: A promising solution to boost performance for vehicular users," *IEEE Communications Magazine*, vol. 51, no. 6, June 2013, pp. 62-68.

[11] D.-T. Phan-Huy and M. Hélard "Large MISO beamforming for high speed vehicles using separate receive & transmit antennas," *IEEE Int. Symposium on Wireless Vehicular Communications,* June 2013.

[12] N. Jamaly, R. Apelfröjd, A. Belén Martinez,, M. Grieger, T. Svensson, M. Sternad and G. Fettweiss, "Analysis and measurement of multiple antenna systems for fading channel prediction in moving relays," *European Conference on Antennas and Propagation (EuCAP 2014)*, April 2014, Hague, The Netherlands.

[13] J. Björsell, M. Sternad and M. Grieger, "Using predictor antennas for the prediction of small-scale fading provides an order-of-magnitude improvement of prediction horizons," *IEEE International Conference on Communications, Workshop WDN-5G ICC2017*, Paris, May 2017.

[14] E. Björnsson, J. Hoydis, M. Kountouris, and M. Debbah, "Massive MIMO systems with non-ideal hardware: Energy efficiency, estimation, and capacity limits," *IEEE Trans. on Information Theory*, vol. 60, no. 11, pp. 7112-7139, Nov. 2014.